

Received: 2018.01.26
Accepted: 2018.03.07
Published: 2018.07.29

Receptor-Interacting Protein 3/Caspase-8 May Regulate Inflammatory Response and Promote Tissue Regeneration in the Periodontal Microenvironment

Authors' Contribution:

Study Design A
Data Collection B
Statistical Analysis C
Data Interpretation D
Manuscript Preparation E
Literature Search F
Funds Collection G

BCEF 1 Bingbing Yan*
D 2 Kewen Wei*
F 3 Lipeng Hou
D 4 Taiqiang Dai
F 5 Yongchun Gu
E 6 Xinyu Qiu
B 7 Jiangwei Chen
D 1 Yuan Feng
B 1 Haode Cheng
F 1 Zhuo Yu
F 8 Yizhe Zhang
AG 2 Hongmei Zhang
A 1 Dehua Li

1 State Key Laboratory of Military Stomatology and National Clinical Research Center for Oral Diseases and Shaanxi Engineering Research Center for Dental Materials and Advanced Manufacture, Department of Oral Implants, School of Stomatology, The Fourth Military Medical University, Xi'an, Shaanxi, P.R. China
2 Department of Burns and Plastic Surgery, Tangdu Hospital, The Fourth Military Medical University, Xi'an, Shaanxi, P.R. China
3 Department of Stomatology, Ninth Hospital, Xi'an, Shaanxi, P.R. China
4 Department of Oral and Maxillofacial Surgery, School of Stomatology, The Fourth Military Medical University, Xi'an, Shaanxi, P.R. China
5 Department of Dentistry, First People's Hospital of Wujiang Dist, Nantong University, Suzhou, Jiangsu, P.R. China
6 Research and Development Center of Tissue Engineering, School of Stomatology, The Fourth Military Medical University, Xi'an, Shaanxi, P.R. China
7 Department of Cardiology, Xijing Hospital, Fourth Military Medical University, Xi'an, Shaanxi, P.R. China
8 Department of Medical Genetics and Developmental Biology, Fourth Military Medical University, Xi'an, Shaanxi, P.R. China

* Both authors contributed equally to this work

Corresponding Authors:

Dehua Li, e-mail: lidehua@fmmu.edu.cn, Hongmei Zhang, e-mail: zzhmei@fmmu.edu.cn

Source of support:

This work was supported by grants from the National Science Foundation of China (NO. 81500857)

Background:

Periodontal ligament stem cells (PDLSCs) possess characteristics of multi-potential differentiation and immunomodulation, and PDLSCs-mediated periodontal tissue regeneration is regarded as a hopeful method for periodontitis treatment. Recent studies demonstrated that RIP3 and caspase8 regulate bacteria-induced innate immune response and programmed necrosis, which is also called necroptosis. This study aimed to determine the role of the RIP3/Caspase8 signal pathway on necroptosis of PDLSCs under the inflammatory microenvironment, both *in vitro* and *in vivo*.

Material/Methods:

PDLSCs were cultured, and transmission electron microscopy and flow cytometry were used to detect necroptosis. PCR, ALP, and Alizarin Red S staining were used to assess the effect of necroptosis on osteogenesis differentiation of PDLSCs *in vitro*, while HE and Masson staining were taken after the nude mouse subcutaneous transplant experiment.

Results:

Our research indicates that RIP3/caspase8 can regulate the immune response of PDLSCs, and blockade of RIP3/caspase8 can protect the biological characteristics of the PDLSCs, effectively promoting periodontal tissue regeneration in the inflammatory microenvironment.

Conclusions:

Inhibiting RIP3/caspase8 can effectively promote periodontal tissue regeneration in the inflammatory microenvironment.

MeSH Keywords:

Necrosis • Periodontal Ligament • Periodontitis • Receptor-Interacting Protein Serine-Threonine Kinases

Full-text PDF:

<https://www.medscimonit.com/abstract/index/idArt/909192>

3318 7 22



Background

Chronic periodontitis is an inflammatory disease associated with periodontal tissue destruction [1,2]. Periodontal ligament stem cells (PDLSCs), possess characteristics of multi-potential differentiation and immuno-modulation, and PDLSCs-mediated periodontal tissue regeneration is now regarded as a promising method for periodontitis treatment [3–5]. Previous *in vitro* studies have demonstrated that PDLSCs can differentiate into cells of periodontal ligament and cementum, and form cementum/periodontal membrane-like structures [6–8]. However, in the inflammatory microenvironment, the ability of PDLSCs to promote multi-potential differentiation and periodontal tissue regeneration is weakened, but the body's immune response is enhanced. The underlying mechanism is still poorly understood [2,9–11].

Necroptosis/programmed necrosis is a newly discovered type of cell death, which exhibits regulated necrotic and apoptotic features [12]. Recent studies proved that necroptosis is mediated by receptor interaction protein 3 (RIP3) and Caspase-8, and eliminating RIP3 can abolish necroptosis [13]. The process of necroptosis needs RIP3 phosphorylation, and mixed lineage kinase domain-like (MLKL) is a downstream protein of RIP3 [14]. RIP3-MLKL can induce necroptosis under lipopolysaccharide (LPS) stimulation, and it regulates the immune response in which IL-1 β participates through NLRP3 (an inflammatory corpuscle) [15]. Previous scholars have demonstrated that necroptosis can participate in the pathology of a number of inflammatory diseases, including periodontitis. Periodontal pathogens may rely on necroptosis to obtain a constant source of substrate for bacterial growth, and the release of DAMPs may induce activation of immune cells and, finally, a comprehensive inflammatory response, leading to periodontal tissue breakdown. On the other hand, necroptosis can release the intracellular bacteria into extracellular microenvironment, which can facilitate immunologic recognition and clearance. Therefore, necroptosis plays an important role in the homeostasis of periodontal tissue [16]. LPS from *Porphyromonas gingivalis* (Pg) is the main pathogenic factor that causes chronic periodontitis [17]. However, whether necroptosis is involved in cell death in the LPS-induced periodontal inflammatory environment remains to be confirmed. Therefore, the present study was designed to explore the role of RIP3/Caspase-8-mediated necroptosis of PDLSCs.

Material and Methods

Cell culture

Freshly-pulled orthodontic tooth were washed in PBS liquid 3–4 times repeatedly. We scraped the periodontal membrane

of the root, and centrifuged scrapings after collection with 3 mg/mL of type I collagen enzyme. After digestion in an incubator at 37°C under 5% CO₂ for 15 min, we added the fetal bovine serum containing α -MEM end-digestion culture. Tissue was cultured in 6-well plates plus 10% fetal bovine serum α -MEM cultures cultured at 37°C and 5% CO₂ in an incubator, changing liquid once every 3 days. Cells at 80% confluence were observed under an inverted microscope.

Reagents and antibodies

LPS was bought from Sigma (St. Louis, MO, USA). Rabbit RIP3, RIP1, MLKL, and β -action antibody were from Proteintech (Chicago, USA). Real-time PCR primer COL1, OCN, RUNX-2, BSP, TNF- α , IL-1 β , IL-18, and GAPDH were from Genecopoeia (USA), and SYBR mixture was from CWBIO Company (China). RT Master Mix was from Takara (Japan). Inhibitor Z-VAD-fmk (ab120382) was from Abcam and GSK'872(2673-5) was bought from BIOVISION. The Annexin V-FITC/PI cell apoptosis detection kit was from Bestbio Company (China). Anti-vimentin antibody (ab8978), Anti-pan Cytokeratin antibody (ab7753), and Alexa Fluor 647(ab150171) were bought from Abcam and Goat Anti-Mouse IgG and Cy3 was bought from Zhuangzhibio (Xi'an, China).

Cell stimulations

This experiment was divided into a control group and experimental groups. PDLSCs were divided into 5 groups: (a) control group: PDLSCs cultured in conventional α -MEM medium for MSCs; (b) LPS group: PDLSCs cultured in medium containing LPS(10 μ g/mL); (c) caspase-8-inhibited group (LPS+Z-VAD-fmk): PDLSCs cultured in medium containing LPS (10 μ g/mL) and Z-VAD-fmk (20 μ M); (d) RIP3-inhibited group (LPS+GSK'872): PDLSCs cultured in medium containing LPS (10 μ g/mL) and GSK'872 (3 μ M); (e) RIP3-inhibited group (LPS+Z-VAD-fmk+GSK'872): PDLSCs cultured in medium containing LPS (10 μ g/mL), Z-VAD-fmk (20 μ M), and GSK'872 (3 μ M).

Real-time quantitative PCR

Inflammatory factors (TNF- α , IL-1 β , IL-18) and those proteins associated with osteogenesis (COL-1, OCN, RUNX-2, BSP) were also detected by real-time PCR. Total RNA was extracted with Trizol reagent (Omega Bio-tek, USA) and cDNA using a PrimeScript RT reagent kit (Takara Biotechnology, Japan). The following primers were used:

COL-1-F: AAGGTGTTGTGCGATGACG,
COL-1-R: CAGACGGGACAGCACTCG;
RUNX-2-F: TGACCATAACCGTCTTCACAA,
RUNX-2-R: GGTTCCCGAGGTCCATCTA;
OCN-F: GAGGGCAGCGAGGTAGTG,
OCN-R: CCTGAAAGCCGATGTGGT,
BSP-F: GAGGGCAGCGAGGTAGTG,

BSP-R: CCTGAAAGCCGATGTGGT;
IL-1 β -F: ACCACCACTACAGCAAGGG,
IL-1 β -R: GGCAGGGAACCAGCATC;
IL-18-F: ACCTGGAATCAGATTACTTTGG,
IL-18-R: ACCTCTAGGCGCTATCTTTA;
TNF- α -F: CGTCTTCTGCCTGCCTGCTG,
TNF- α -R: GCTTGTCCTCGGGGTTT.
GAPDH mRNA as an internal reference and the SYBR Mixture (CW BIO Company, China) were used for real-time PCR.

Western blotting

The cells were cultured in 6-well plates and treated with indicated stimuli, and the protein samples were prepared by following the protein extraction kit instructions. The total protein was selected after centrifugation and it was measured with the BCA protein assay kit (Pierce Biotechnology, USA). We loaded 30 μ g of total proteins on 12% SDS-PAGE and transferred it to a PVDF membrane (Millipore, USA), and then blocked it in 5% BSA for 1 h at room temperature. The appropriate primary antibodies were added to the membranes. After rinsing in Tris-buffered saline 3 times, the membranes were incubated by the appropriate secondary antibodies for 1 h at room temperature. The blots were captured by use of the Western-Light Chemiluminescent Detection System (Tanon, China).

Transmission electron microscopy

The specimens were fixed with glutaraldehyde and then sent to the electron microscopy center. The samples were prepared for conventional electron microscopy, and the samples were dehydrated, permeated, and treated with lead and uranium. The specimens were observed under a transmission electron microscope (JEOL-1230, LSCM, Hitachi, Japan).

Quantitative analysis of apoptosis

The apoptosis and the degree of apoptosis were evaluated by Annexin V and PI double staining following instructions of the kit (Bestbio, China). Flow cytometry (FCM) can distinguish and quantify 4 cell subgroups, including necrotic cells (Annexin-/PI+), normal living cells (Annexin-/PI-), early apoptotic cells (Annexin+/PI-), and late apoptotic cells (Annexin+/PI+).

In vitro osteogenic assay

For osteogenic differentiation, the cells (P4) were seeded in 6-well plates at a density of 4×10^4 cells/per well, which aimed to quantify mineralized nodule formation *in vitro*. The cells were incubated in medium supplemented with 10% FBS. The medium was then switched to osteogenic differentiation medium, which contains 0.1 mM dexamethasone, 10 mM β -glycerophosphate, 50 mg/mL ascorbate phosphate (all from Sigma

Aldrich), and 10% FBS. The medium was changed every 2 days. Mineralization was detected and quantified using an Alizarin Red, and 4 wells were analyzed for each group. The quantification assay was performed using an ALP activity detection kit (Jiancheng Bioengineering, Nanjing, China). The cells were fixed with 4% paraformaldehyde for 20 min and stained with 2% Alizarin Red (PH 4.2) (Kermel, Tianjin, China). The mineralized nodules were dissolved by hexadecyl pyridinium chloride and isopropanol, and quantitative absorbance was measured at 560nm for statistical analysis.

Enzyme-linked immunosorbent assay (ELISA)

TNF- α , IL-1 β , and IL-18 ELISA kits were bought from Nanjing Jiancheng Bioengineering Institute (Nanjing, China). The cytokine levels were measured according to the manufacturer's guidelines. Each sample was analysed in duplicate.

Flow cytometry analysis

Cell phenotypes of early passages (P2) of cultured cells were detected by flow cytometry analysis to measure the expression of stem cell surface markers [18]. Approximately 1×10^6 PDLSCs adherent cells were harvested. Then, the single-cell suspension was re-suspended and incubated with antibodies for human CD146 (PE), STRO-1 (APC) (BD Bioscience, San Jose, CA, USA) at 4°C. The samples were measured by flow cytometry analysis using a BD FACS Arial cytometer (BD FACS, CA, USA), and the experiment was repeated 3 times.

Induction of PDLSCs-CA

A total of 3×10^4 PDLSCs were seeded into a 6-well plate and cultured in α -MEM containing 10% FBS until the cells reached 80% confluence. Then, the medium was changed to α -MEM (10% FBS) containing 50 μ g/mL vitamin C (VC), and it was refreshed every 2 days. After about 10 days, a white membrane structure could be observed and CA became thicker with time.

Morphological observation of cell aggregate

Harvested PDLSCs-CA cells were fixed with 4% paraformaldehyde overnight and the microstructure of the resultant cell sheets were examined by scanning electron microscopy (SEM, Hitachi S-4300; Tokyo, Japan). Briefly, after being washed in PBS 3 times, cell sheets were fixed with 2.5% glutaraldehyde at 0°C, dehydrated, and dried in a critical-point dryer. The experiment was repeated 4 times.

In vivo transplantation and histomorphometric analysis

PDLSCs-CA mixed with 20 mg Bio-Oss spongiouse bone substitute particles (Geistlich, Switzerland) were subcutaneously

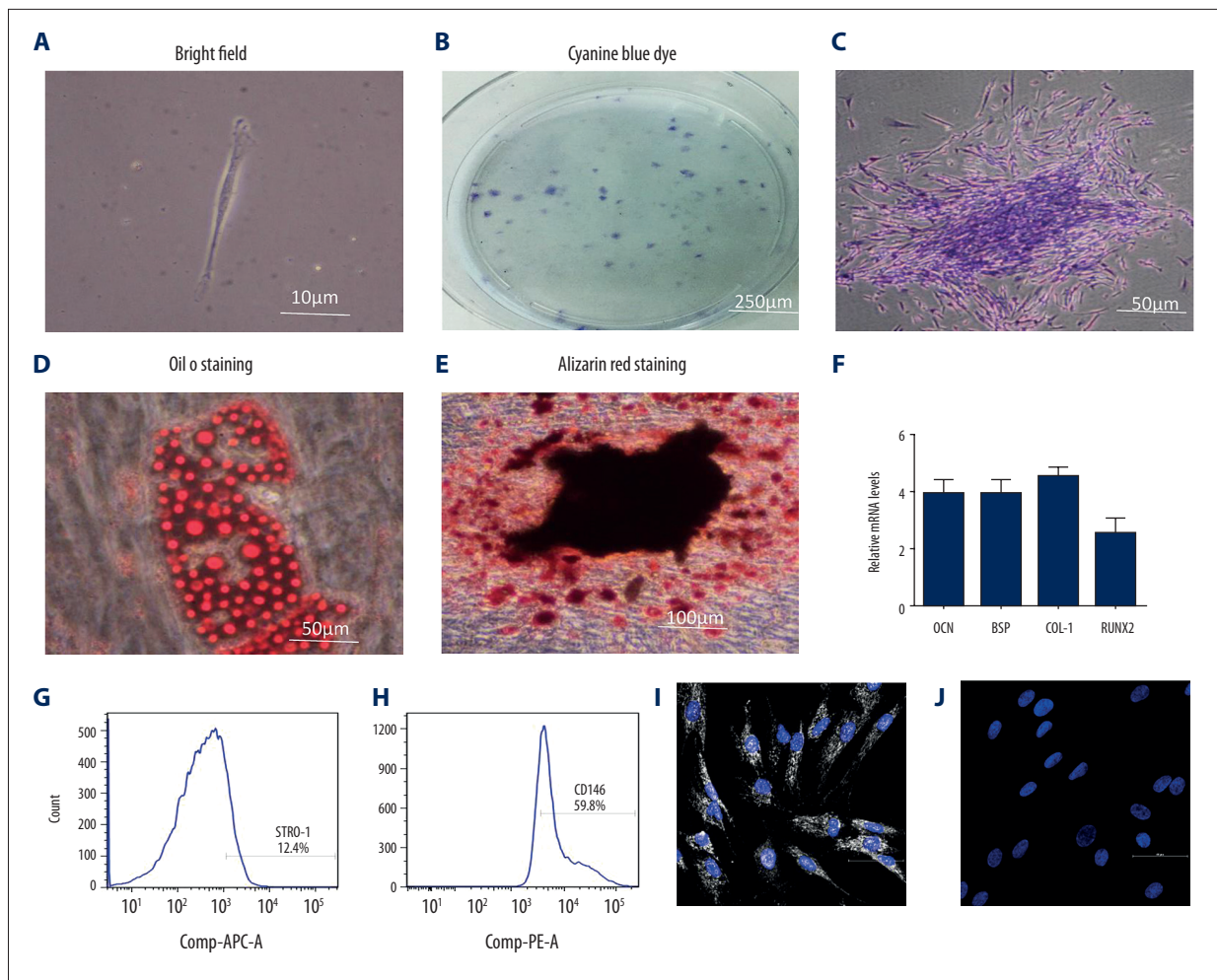


Figure 1. PDLSCs culture and identification ((A) single PDLSC; (B) A clone of the cyanine blue dye PDLSCs; (C) PDLSCs Polyclonal formation; (D) PDLSCs lipid droplet formed after lipid induction, oil red O staining positive; (E) mineralized nodules formed after PDLSCs were osteo-induced, and Alizarin Red staining was positive; (F) RT-PCR after mineralized induction, PDLSCs expressed osteogenic proteins (COL1, OCN, RUNX-2, BSP); (G, H) Flow cytometry detection of the mesenchymal stem cell marker of PDLSCs was tested positive for STRO-1 and CD146; (I, J) Cultured cells were identified by immunofluorescence technology staining using anti-vimentin monoclonal antibody and cytokeratin polyclonal antibody.

implanted into the dorsal region of immunocompromised mice (male, 7–9-week-old; Fourth Military Medical University Animal Center, Xi'an, China) (3 animals per testing group) to further investigate the biocompatibility of PDLSCs-CA *in vivo*. All animal procedures complied with the guidelines of the Fourth Military Medical University Intramural Animal Use and Care Committee, and also met the NIH guidelines for the care and use of laboratory animals in this study. The nude mice were sacrificed at 8 weeks post-surgery and the excised specimens were fixed in 4% neutral formaldehyde. Then, scanning electron microscopy (SEM, Hitachi S-4300; Tokyo, Japan) was used to observe the microstructure of the resultant cell PDLSCs-CA, Bio-Oss scaffold, and the excised specimens. The harvested samples were decalcified in 17% EDTA solution for 2 weeks and embedded in paraffin. Then, the samples were sectioned horizontally every

5 µm, and were subjected to H&E and Masson staining to locate the area. The formation and organization of regenerated tissues were observed using light and polarized microscopy (BX50, Olympus Optical) and were evaluated from at least 3 randomly selected fields from each specimen with Image Pro Plus 6.0 software. New cementum was defined as the mineralized tissue formed with collagen bundles similar to the Sharpey's fibers inserted. The percentage of new cementum was equal to the ratio of the length of new cementum to the length of the whole area.

Statistical analysis

Data are shown as means \pm SEM. The statistical results were analyzed by GraphPad Prism 6 software. One-way analysis of

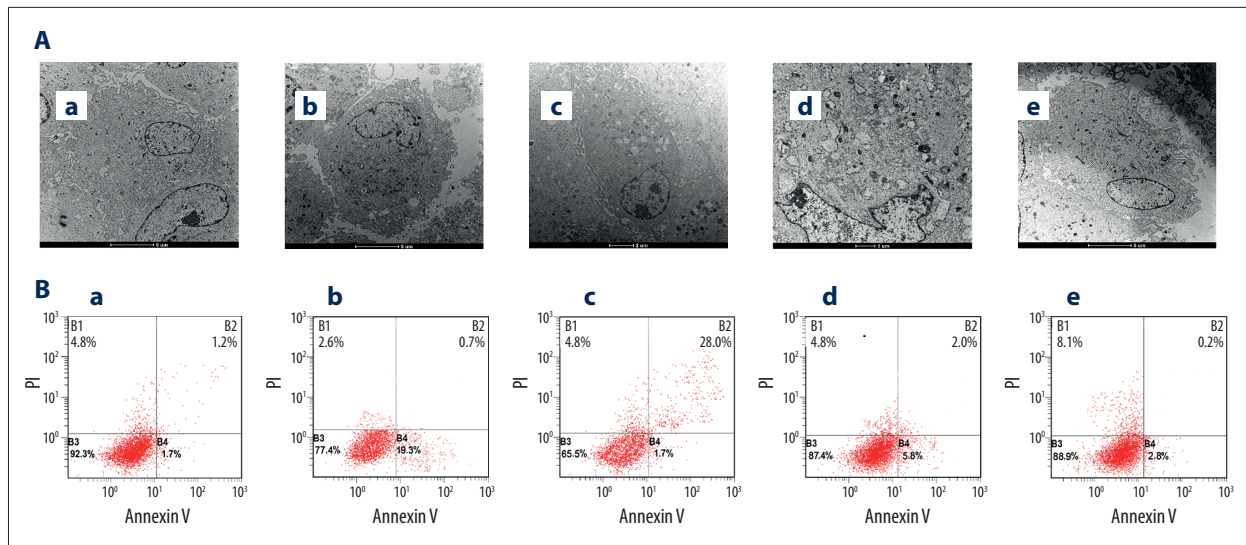


Figure 2. Necroptosis is involved in cell death of inflammatory PDLSCs. (A) Some representative TEM images of PDLSC in different forms of cell death: (a) normal PDLSCs, (b) necroptosis PDLSCs, (c) necroptosis PDLSCs, (d) apoptosis PDLSCs, and (e) rehabilitation PDLSCs. (B) Annexin V, PI/FITC Flow cytometry analysis of the PDLSCs: (a) Control group; (b) LPS group; (c) LPS+Z-VAD-fmk group; (d) LPS+GSK'872 group; (e) LPS+Z-VAD-fmk+GSK'872 group.

variance followed by the Bonferroni's post hoc test was used to compare groups. Statistical significance was set at $p < 0.05$.

Results

PDLSCs culture and identification

Clonal cultured PDLSCs had multi-directional differentiation ability – osteogenic and adipogenic differentiation – and they expressed the mesenchymal stem cell marker STRO-1 and CD146. After mineralization induction, the expression of osteogenic proteins COL1, OCN, RUNX-2, and BSP could be detected by RT-PCR. Anti-vimentin monoclonal antibody immunofluorescence technology staining was positive and cytokeratin staining was negative. All of these results showed that PDLSCs were consistent with the characteristics of mesenchymal source (Figure 1).

Necroptosis was involved in cell death of PDLSCs in an inflammatory microenvironment

After cells were stimulated for 24 h, the cellular ultrastructure of the PDLSCs was examined by TEM to determine the patterns of cell death. The PDLSCs displayed normal cellular ultrastructure in the control group, whereas in the LPS-stimulating group and the caspase-8 inhibited group, the cells exhibited characteristics of necroptosis, including rupture of cell membrane, organelle disappearance, chromatin solidification, and agglutination. Apoptosis was detected in the RIP3-inhibited group with LPS and GSK'872, which was characterized by cytoplasmic retraction, chromatin edge set, nuclear fixation, nuclear

DNA fracture, and formation of apoptosis body. However, the RIP3- and caspase8-inhibited group (LPS+Z-VAD-fmk+GSK'872) showed only a mild degree of necrosis: cell membranes and organelles were complete, the nucleus was round, and the cellular structure was not destroyed (Figure 2A).

Under the Pg-LPS stimulation, caspase-8 inhibitors in the environment were cultivated with PDLSCs for 48 h, followed by collecting cells, PI/Annexin V dyeing, and flow cytometry instrument testing. The results showed that, under the Pg-LPS stimulation, cell death increased after caspase-8 inhibition, cell death was relieved after RIP3 inhibitor was inhibited. The results showed that PDLSCs underwent necroptosis in the inflammatory microenvironment, as shown in Figure 2B.

RIP3/caspase8 regulated the signal of PDLSCs in the inflammatory environment

Pg-LPS (10 $\mu\text{g}/\text{mL}$ -stimulated PDLSCs were cultured for 24 h after adding RIP3/caspase-8 signal inhibitor, followed by protein extraction. Western blot (WB) analysis showed that, after Pg-LPS stimulates PDLSCs, RIP1 and RIP3 are expressed, RIP3 expression is enhanced after caspase-8 is inhibited, and RIP3 inhibitor GSK'872 can effectively suppress RIP3 expression, as shown in Figure 3.

In the inflammatory microenvironment, RIP3/caspase8 regulated the biological characteristics of PDLSCs.

PDLSCs were cultured in an *in vitro* inflammatory environment. RIP3/caspase-8 signal inhibition and the osteo-induction

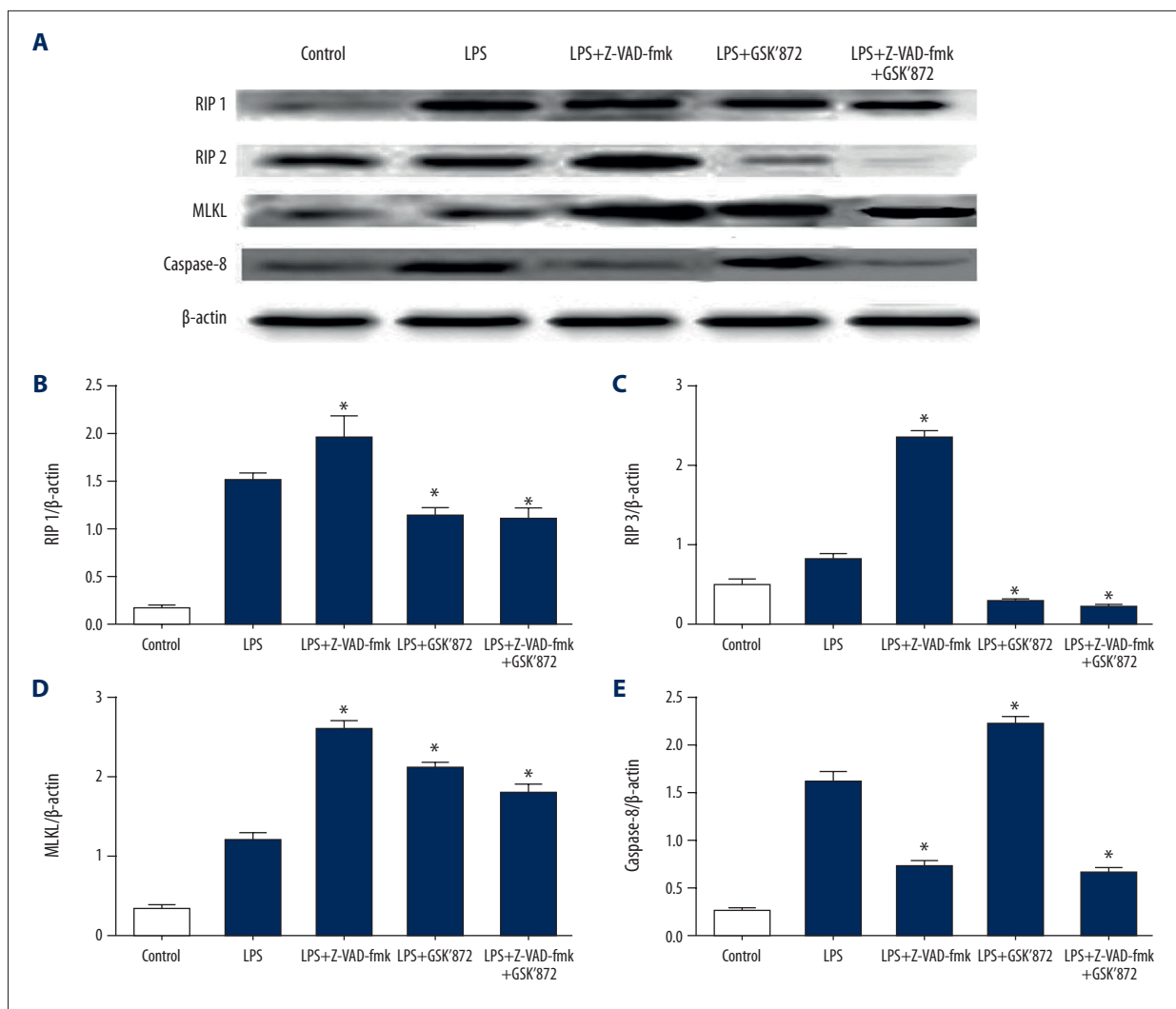


Figure 3. Western blot RIP1, RIP3, MLKL, and caspase-8 expression in inflammatory environment (Z-VAD-fmk: caspase-8 inhibitor; GSK'872: RIP3 inhibitor) * $P < 0.05$ vs. LPS group.

solution were added to detect the osteogenesis differentiation of PDLSCs, and the expression level of the related osteogenic genes in osteogenic differentiation was determined by real-time PCR (Figure 4A). After being cultured in osteo-inductive medium for 21 days, mineralized extracellular matrices were observed in PDLSCs, as demonstrated by Alizarin Red staining (Figure 4B). After being cultured in osteo-inductive medium for 7 days, PDLSCs showed increased ALP colonies (Figure 4C). Quantitative analysis showed that PDLSCs had lower osteogenic potential under chronic inflammatory conditions (Figure 4D, 4E), especially in necroptosis situations.

RIP3/caspase8 regulates the immune response of PDLSCs in the inflammatory environment

RT-PCR results show that TNF- α , IL-1 β , and IL-18 levels increase after the Pg-LPS stimulate PDLSCs, and the level keeps rising

after caspase-8 is inhibited. However, it is reduced after RIP3 is inhibited. The results showed that RIP3/caspase-8 regulates the immune response of PDLSCs in the inflammatory environment (Figure 5A). In periodontal inflammatory microenvironment, pro-inflammatory cytokines mediate the inflammatory response to LPS and promote damage to the periodontal tissues. Necrosis is connected with a high level of pro-inflammatory cytokines [18–20]. Therefore, the levels of classical pro- and anti-inflammatory cytokines TNF- α , IL-1 β , and IL-18 were measured. As shown in Figure 5B, ELISA indicated LPS treatment significantly increased TNF- α , IL-1 β , and IL-18 levels in the LPS-treated groups.

Biocompatibility of PDLSCs-CA+Bio-Oss *in vivo*

The scaffold material, Bio-Oss (Figure 6B), combined with PDLSCs-CA (Figure 6C), was subcutaneously transplanted into

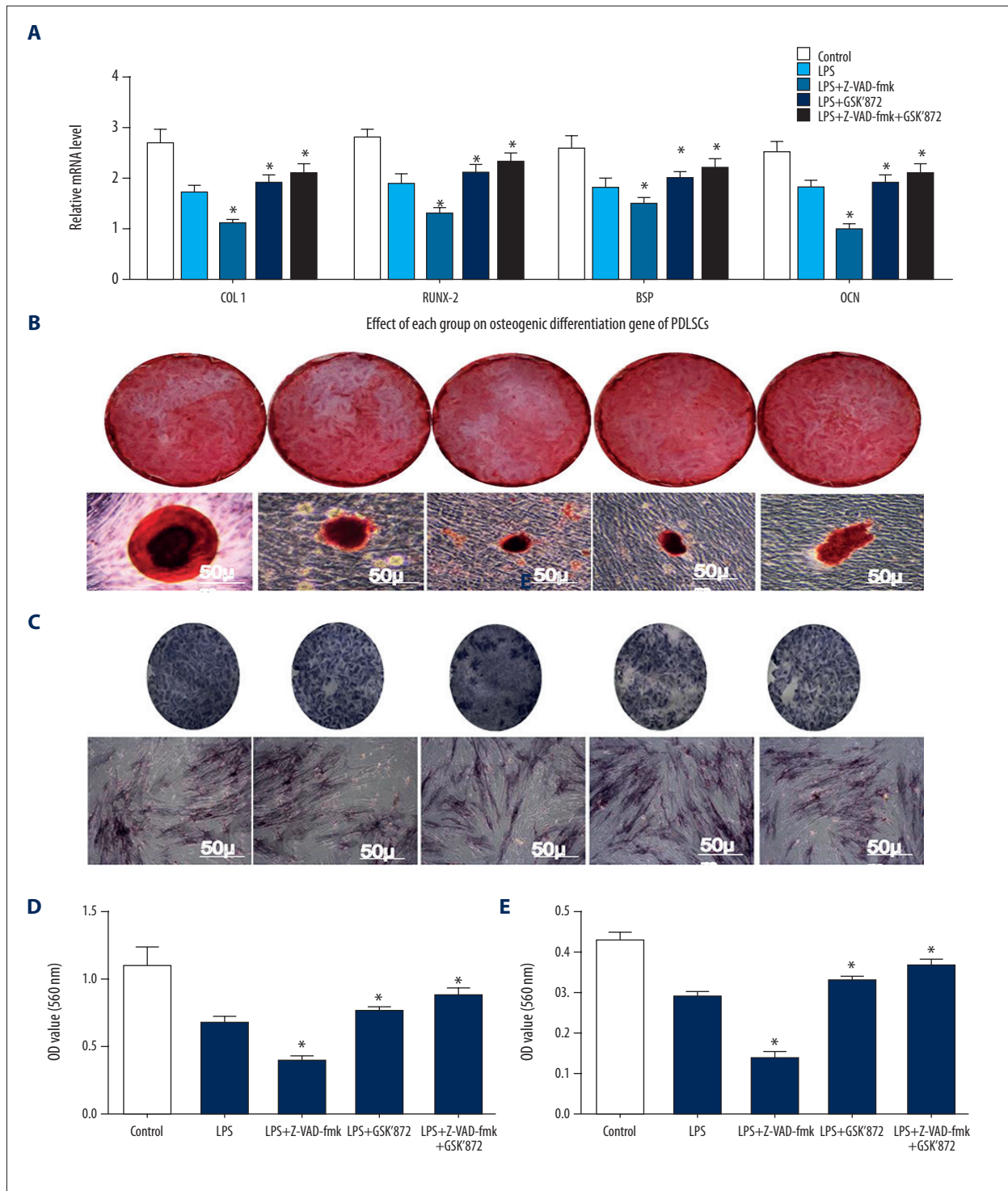


Figure 4. *In vitro* osteogenic assay. (A) the relative mRNA levels of osteogenesis-related gene. (B) Cultured PDLSCs formed calcified nodules that stained positively for Alizarin Red S staining after 3 weeks of osteogenic induction. (C) Representative images of alkaline phosphatase (ALP) staining in PDLSCs treated by osteogenic induction medium for 7 days. (D) Quantitative comparison of mineralized nodule formation. (E) Quantitative analysis of ALP activity in PDLSCs. * $p < 0.05$ vs. LPS group.

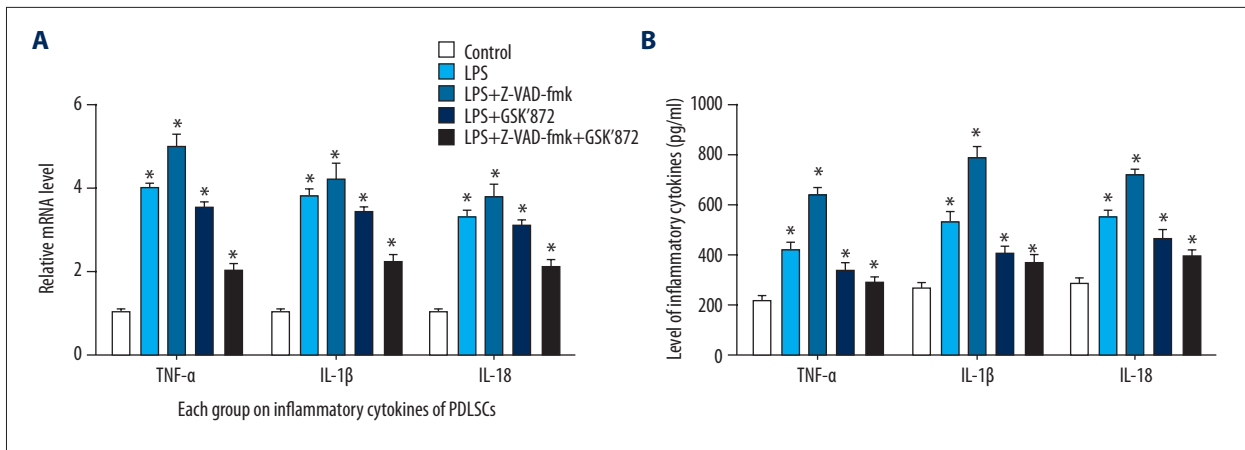


Figure 5. Inflammatory cytokines. (A) Relative mRNA levels of inflammatory cytokines associated with periodontal inflammatory microenvironment. (B) Concentration of TNF-α, IL-1β, and IL-18 in serum. * p<0.05 versus LPS group.

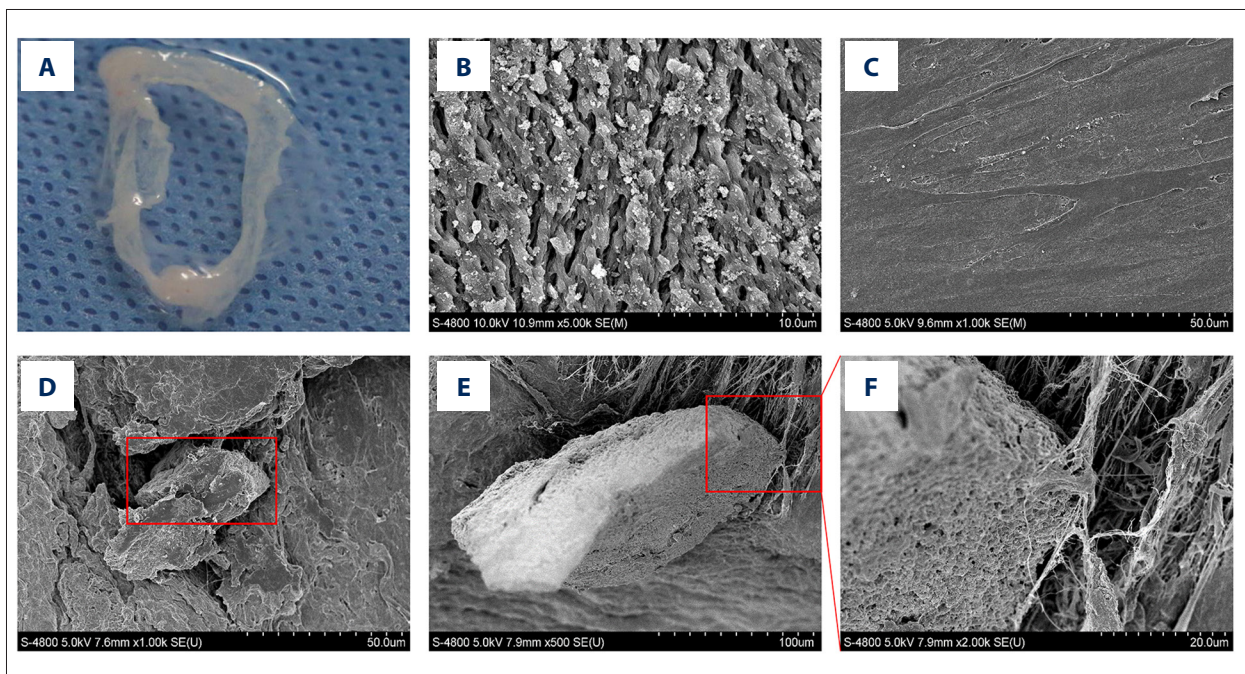


Figure 6. Cell aggregates (A, C) and Bio-Oss (B) particles were combined and subcutaneously implanted into immunocompromised mice as indicated by SEM images of the specimens of the PDLSCs-CA (D-F).

the dorsal region of immunocompromised mice to assess the biocompatibility. At 8 weeks after transplantation, SEM examination (Figure 6D–6F) showed that they have good biocompatibility *in vivo*.

The regeneration of periodontal tissue of PDLSCs in inflammatory state can be effectively promoted through inhibiting RIP3/caspase8

Compared to the control group, the LPS group generated less newly formed cementum at 8 weeks after surgery (Figure 7A) (p<0.05). However, the composition of cementum in the RIP3/

caspase-8 inhibition group (Figure 7Ae) was significantly higher than that of the other inflammatory groups (Figure 7Ab–d). In the present study, we used Image Pro Plus 6.0 software to scan the bone area of 3 random fields and compared the area values (Figure 7B). The results showed that the ability of the stem cells to form heterotopic cementum in an inflammatory environment was significantly decreased (p<0.05), and inhibiting RIP3/caspase-8 effectively inhibited this decrease.

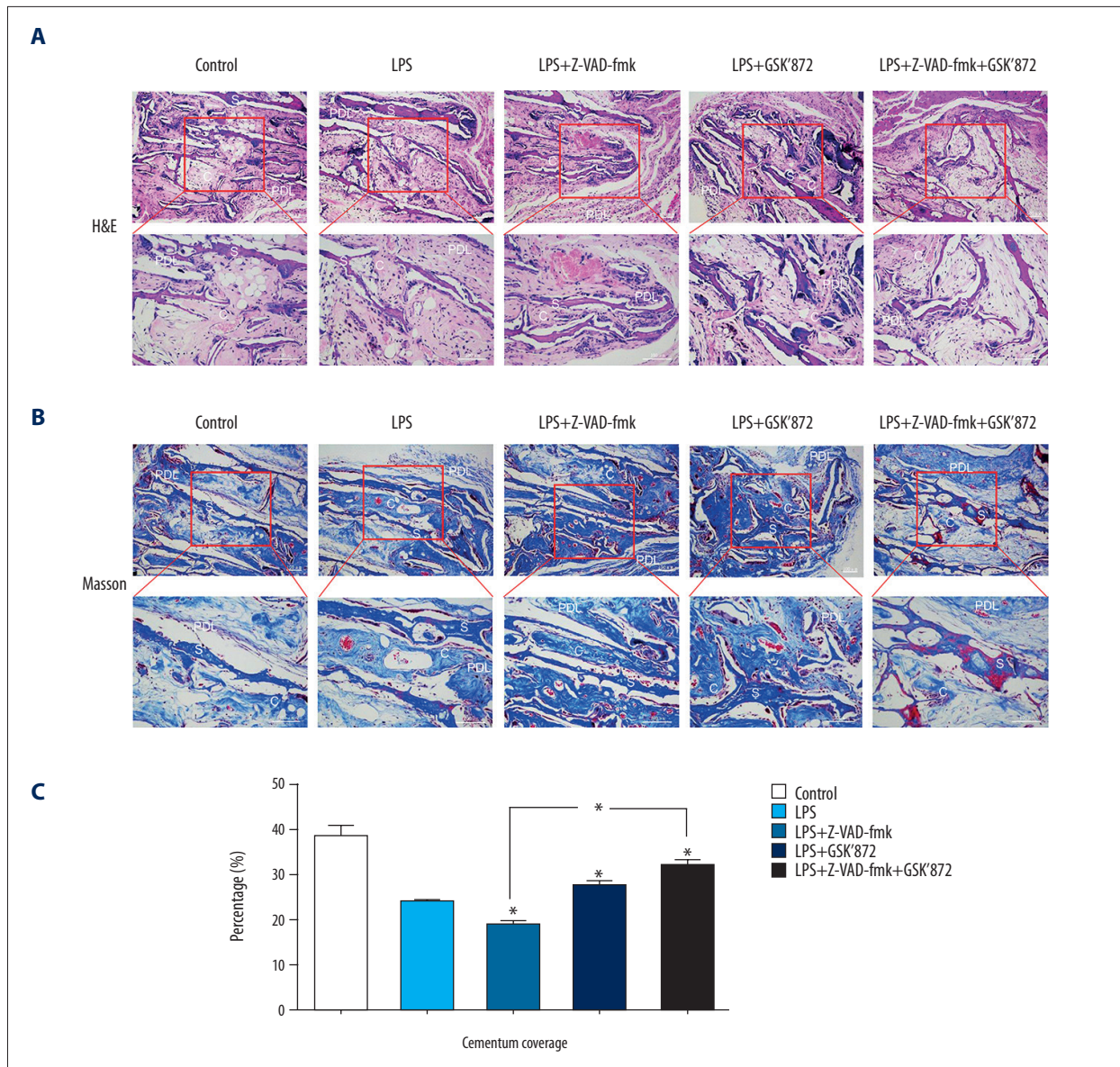


Figure 7. Histomorphometric analysis of the newly formed cementum-like mineralized deposits tissues. Representative hematoxylin and eosin (H&E) and Masson staining indicated the formation of cementum and periodontal ligament fibers at 8 weeks after surgery (A, B). (C) The corresponding quantitative analysis of histomorphometry observation. c – cementum; s – scaffold; pdl – periodontal ligament. * p<0.05 versus LPS group.

Discussion

Traditionally, apoptosis and necrosis are regarded as the 2 main forms of cell death involved in the regulation of periodontitis [18]. Necroptosis, also called programmed necrosis, is a newly discovered form of programmed cell death, which exhibits characteristics of both apoptosis and necrosis and plays important roles in severe tissue injury, including periodontal disease. Recent studies showed that necroptosis is strongly associated with periodontitis [12,14,19]. However, the mechanism whereby necroptosis induces periodontitis is still unclear.

Studies have shown that the process of necroptosis needs RIP3 phosphorylation, while MLKL is a downstream protein of RIP3.

Necroptosis can be induced by various stimuli, including LPS, which has been studied most extensively, as well as Toll-like receptors, intracellular RNA and DNA sensors, and many other mediators. Necroptosis requires the assembly of RIP1/RIP3 necrosome. Upon activating the TNF receptor, mutual direct and indirect phosphorylation of RIP1 and RIP3 in the necrosome activates necrotic signal pathway, whereas caspase-8, a cysteine protease which is critically involved in regulation of cellular

apoptosis, is inhibited during this process. Caspase-8 is known as the beginning caspase in apoptosis pathway, which can directly activate the downstream effect of caspases. In some cells, programmed necrosis can occur directly under the mediation of the death receptor because the caspase activity is weak. However, programmed necrosis can occur when Z-VAD-fmk inhibit caspase activity in the cells whose caspase activity is stronger. This is because the activation caspase-8 can restrain diubiquitin localization process of RIP1 by shear CYLD, thereby inhibiting programmed necrosis. RIP3 can regulate inflammatory bodies and strengthen the inflammatory response in caspase-8 defects, and at the same time, caspase-8 has dual functions on RIP3 in regulating inflammation reaction, in which necroptosis is mediated by RIP3, and the release of inflammatory cytokines after cell necrosis are inhibited by caspase-8. On the other hand, the activation of NLRP3 inflammatory bodies, which RIP3 mediated, as well as the production of IL-1 β , are also activated by caspase-8 [20,21].

PDLSCs were cultured and identified (Figure 1), which could prove they were from the mesenchymal stem cells. TEM (Figure 2A) is the criterion standard for judging necroptosis, which can be blocked by inhibiting RIP3 (Figure 2B). The above studies showed that necroptosis occurred in PDLSCs. The primary role of RIP3 is to induce necroptosis, and promoting the inflammatory response is thought to be the second level, since the release of a dangerous related molecular model is made up of dead cells secreting, which is the main driving force of inflammation in physiologic necrosis. RIP3 can also directly promote inflammation through the production of inflammatory cytokines [22]. In the second group, the protein expression levels of caspase-8 was higher than in the normal group, indicating that PDLSCs had apoptosis, while RIP1, RIP3, and MLKL had different degrees of expression, indicating that a small number of PDLSCs had necroptosis. RIP1, RIP3, and MLKL expression was higher in the third group, showing that PDLSCs increase necroptosis. RIP3 was inhibited in the fourth group, while caspase-8 expression was higher than the third group. These results demonstrate that PDLSCs may have transitioned from necroptosis to apoptosis. RIP1 and MLKL expression were lower in the last group than in the fourth group, showing that necroptosis was inhibited more severely after apoptosis was also inhibited (Figure 3). ALP, Alizarin Red staining, ALP, and Alizarin Red activity quantification indicated that the osteogenesis differentiation ability of PDLSCs declined in inflammatory conditions, which is in accordance with the results of the RT-PCR. After necroptosis occurred, PDLSCs osteogenesis ability decreased significantly, while the downward trend had a certain degree of recovery after RIP3/caspase-8 was inhibited. Therefore, inhibiting RIP3/caspase-8 may play a protective role in biological characteristics of PDLSCs (Figure 4). Various inflammatory factors were

highly expressed in PDLSCs in inflammatory conditions, which showed that RIP3/caspase-8 regulates the PDLSC immune response (Figure 5A); inflammatory factor expression level increased after caspase-8 was inhibited and the level decreased after RIP3 was inhibited, suggesting that this effect was caused by necroptosis, and it further illustrates that inhibiting RIP3/caspase-8 can reduce the inflammatory reaction and immune characteristics of PDLSCs (Figure 5B). These findings, together with the fact that RIP3/caspase-8 is essential for the induction of necroptosis, indicate that RIP3/caspase-8-dependent necroptosis promoted the LPS-induced periodontal inflammatory microenvironment through enhancing inflammation.

The *in vitro* and *in vivo* results showed that PDLSCs-CA and Bio-Oss had strong biocompatibility, which created favorable conditions for heterotopic transplantation *in vivo* (Figure 6). One of our aims was to assess periodontal tissue regeneration in the inflammatory microenvironment, and the *in vivo* results demonstrated PDLSCs could form new cementum, and inhibiting RIP3/caspase-8 can raise periodontal regeneration expectations (Figure 7). So, our study provides new prospects for treating periodontitis in the future.

RIP1 is a key regulatory factor for necroptosis, and RIP3 is a specific protein factor. The research showed that apoptosis and necroptosis can be converted to each other, and RIP3 is a molecular "switch" that can affect the transformation of energy metabolism by regulating it. It also suggests that it is necessary to block both apoptosis and necroptosis to achieve satisfactory results in treatment. This is the first article on the necroptosis of PDLSCs.

Conclusions

In summary, *in vitro* and *in vivo* experiments demonstrated that RIP3/caspase-8 can regulate the inflammatory reaction of PDLSCs, and inhibiting RIP3/caspase-8 can promote periodontal tissue regeneration in the inflammatory microenvironment.

Acknowledgments

We would like to thank Yan Zhao at Yan Chang Petrol for his polishing of this article, and Bingbing Yan is especially grateful to his wife Liang Zhao, who accompanied by him in the dim light every night when he was writing this article.

Conflict of interest

None.

References:

1. Hu DY, Hong X, Li X: Oral health in China – trends and challenges. *Int J Oral Sci*, 2011; 3: 7–12
2. Kato H, Taguchi Y, Tominaga K et al: Porphyromonas gingivalis LPS inhibits osteoblastic differentiation and promotes pro-inflammatory cytokine production in human periodontal ligament stem cells. *Arch Oral Biol*, 2014; 59: 167–75
3. Seo BM, Miura M, Gronthos S et al: Investigation of multipotent postnatal stem cells from human periodontal ligament. *Lancet*, 2004; 364: 149–55
4. Moriwaki K, Bertin J, Gough PJ, Chan FK: A RIPK3-caspase 8 complex mediates atypical pro-IL-1beta processing. *J Immunol*, 2015; 194: 1938–44
5. Izawa A, Ishihara Y, Mizutani H et al: Inflammatory bone loss in experimental periodontitis induced by *Aggregatibacter actinomycetemcomitans* in interleukin-1 receptor antagonist knockout mice. *Infect Immun*, 2014; 82: 1904–13
6. Kinney JS, Morelli T, Oh M et al: Crevicular fluid biomarkers and periodontal disease progression. *J Clin Periodontol*, 2014; 41: 113–20
7. Menicanin D, Mrozik KM, Wada N et al: Periodontal-ligament-derived stem cells exhibit the capacity for long-term survival, self-renewal, and regeneration of multiple tissue types *in vivo*. *Stem Cells Dev*, 2014; 23: 1001–11
8. Zhang J, Li ZG, Si YM et al: The difference on the osteogenic differentiation between periodontal ligament stem cells and bone marrow mesenchymal stem cells under inflammatory microenvironments. *Differentiation*, 2014; 88: 97–105
9. Li C, Li B, Dong Z et al: Lipopolysaccharide differentially affects the osteogenic differentiation of periodontal ligament stem cells and bone marrow mesenchymal stem cells through Toll-like receptor 4 mediated nuclear factor kappaB pathway. *Stem Cell Res Ther*, 2014; 5: 67
10. Humphries F, Yang S, Wang B, Moynagh PN: RIP kinases: Key decision makers in cell death and innate immunity. *Cell Death Differ*, 2015; 22: 225–36
11. Seo T, Cha S, Kim TI et al: Porphyromonas gingivalis-derived lipopolysaccharide-mediated activation of MAPK signaling regulates inflammatory response and differentiation in human periodontal ligament fibroblasts. *J Microbiol*, 2012; 50: 311–19
12. Pasparakis M, Vandenabeele P: Necroptosis and its role in inflammation. *Nature*, 2015; 517: 311–20
13. Rayamajhi M, Miao EA: The RIP1-RIP3 complex initiates mitochondrial fission to fuel NLRP3. *Nat Immunol*, 2014; 15: 1100–2
14. Tsuda H, Ning Z, Yamaguchi Y, Suzuki N: Programmed cell death and its possible relationship with periodontal disease. *J Oral Sci*, 2012; 54: 137–49
15. Huang MT, Taxman DJ, Holley-Guthrie EA et al: Critical role of apoptotic speck protein containing a caspase recruitment domain (ASC) and NLRP3 in causing necrosis and ASC speck formation induced by *Porphyromonas gingivalis* in human cells. *J Immunol*, 2009; 182: 2395–404
16. Li J, Ke XJ, Yan F et al: Necroptosis in the periodontal homeostasis: Signals emanating from dying cells. *Oral Disease*, 2017 [Epub ahead of print]
17. Gurung P, Kanneganti TD: Novel roles for caspase-8 in IL-1beta and inflammasome regulation. *Am J Pathol*, 2015; 185: 17–25
18. Tsuda H, Ochiai K, Suzuki N, Otsuka K: Butyrate, a bacterial metabolite, induces apoptosis and autophagic cell death in gingival epithelial cells. *J Periodontol Res*, 2010; 45: 626–34
19. Shangase SL, Mohangi GU, Hassam-Essa S, Wood NH: The association between periodontitis and systemic health: An overview. *SADJ*, 2013; 68: 10–12
20. Dinarello CA: Interleukin-1 in the pathogenesis and treatment of inflammatory diseases. *Blood*, 2011; 117: 3720–32
21. Hao L, Li JL, Yue Y et al: Application of interleukin-1 genes and proteins to monitor the status of chronic periodontitis. *Int J Biol Markers*, 2013; 28: 92–99
22. Lamkanfi M, Dixit VM: Mechanisms and functions of inflammasomes. *Cell*, 2014; 157: 1013–22